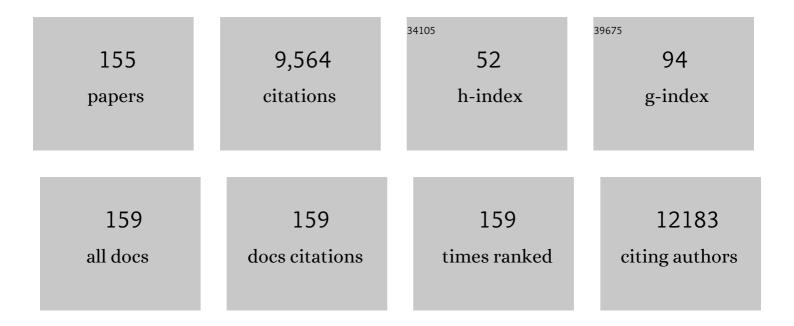
Yeon Sik Jung

List of Publications by Year in descending order

Source: https://exaly.com/author-pdf/6085099/publications.pdf Version: 2024-02-01



YEON SIK LUNC

#	Article	IF	CITATIONS
1	Modulation and Modeling of Threeâ€Dimensional Nanowire Assemblies Targeting Gas Sensors with High Response and Reliability. Advanced Functional Materials, 2022, 32, 2108891.	14.9	6
2	Metal oxide charge transfer complex for effective energy band tailoring in multilayer optoelectronics. Nature Communications, 2022, 13, 75.	12.8	9
3	Comparative Study of Thermoelectric Properties of Sb ₂ Si ₂ Te ₆ and Bi ₂ Si ₂ Te ₆ . ACS Applied Materials & Interfaces, 2022, 14, 1270-1279.	8.0	15
4	Separation-free bacterial identification in arbitrary media via deep neural network-based SERS analysis. Biosensors and Bioelectronics, 2022, 202, 113991.	10.1	27
5	Selfâ€Induced Solutal Marangoni Flows Realize Coffeeâ€Ringâ€Less Quantum Dot Microarrays with Extensive Geometric Tunability and Scalability. Advanced Science, 2022, 9, e2104519.	11.2	15
6	Modulation and Modeling of Threeâ€Dimensional Nanowire Assemblies Targeting Gas Sensors with High Response and Reliability (Adv. Funct. Mater. 10/2022). Advanced Functional Materials, 2022, 32, .	14.9	0
7	Polychromatic Quantum Dot Array to Compose a Community Signal Ensemble for Multiplexed miRNA Detection. ACS Nano, 2022, 16, 11115-11123.	14.6	15
8	High-Capacity Ti ₃ C ₂ T _{<i>x</i>} MXene Electrodes Achieved by Eliminating Intercalated Water Molecules Using a Co-solvent System. ACS Applied Materials & Interfaces, 2022, 14, 30080-30089.	8.0	2
9	Heat-fueled enzymatic cascade for selective oxyfunctionalization of hydrocarbons. Nature Communications, 2022, 13, .	12.8	17
10	A Systematic Study of the Interactions in the Top Electrode/Capping Layer/Thin Film Encapsulation of Transparent OLEDs. Journal of Industrial and Engineering Chemistry, 2021, 93, 237-244.	5.8	6
11	Order-disorder transition-induced band nestification in AgBiSe ₂ –CuBiSe ₂ solid solutions for superior thermoelectric performance. Journal of Materials Chemistry A, 2021, 9, 4648-4657.	10.3	22
12	High-performance ultracapacitor electrodes realized by 3-dimensionally bicontinuous block copolymer nanostructures with enhanced ion kinetics. Journal of Materials Chemistry A, 2021, 9, 16119-16128.	10.3	2
13	Universal vertical standing of block copolymer microdomains enabled by a gradient block. Journal of Materials Chemistry C, 2021, 9, 14021-14029.	5.5	3
14	Vertically aligned nanostructures for a reliable and ultrasensitive SERS-active platform: Fabrication and engineering strategies. Nano Today, 2021, 37, 101063.	11.9	43
15	Hierarchically layered nanocomposite electrodes formed by spray-injected MXene nanosheets for ultrahigh-performance flexible supercapacitors. Applied Surface Science, 2021, 549, 149226.	6.1	14
16	Extreme-Pressure Imprint Lithography for Heat and Ultraviolet-Free Direct Patterning of Rigid Nanoscale Features. ACS Nano, 2021, 15, 10464-10471.	14.6	10
17	Conformation-modulated three-dimensional electrocatalysts for high-performance fuel cell ell ell ell ell ell ell	10.3	27
18	Synergistic SERS Enhancement in GaNâ€Ag Hybrid System toward Labelâ€Free and Multiplexed Detection of Antibiotics in Aqueous Solutions. Advanced Science, 2021, 8, e2100640.	11.2	28

#	Article	IF	CITATIONS
19	Regulating Te Vacancies through Dopant Balancing via Excess Ag Enables Rebounding Power Factor and High Thermoelectric Performance in pâ€Type PbTe. Advanced Science, 2021, 8, e2100895.	11.2	18
20	Synergistic Integration of Chemoâ€Resistive and SERS Sensing for Labelâ€Free Multiplex Gas Detection. Advanced Materials, 2021, 33, e2105199.	21.0	25
21	Microcellular sensing media with ternary transparency states for fast and intuitive identification of unknown liquids. Science Advances, 2021, 7, eabg8013.	10.3	3
22	Controlling hot electron flux and catalytic selectivity with nanoscale metal-oxide interfaces. Nature Communications, 2021, 12, 40.	12.8	20
23	Unconventional grain growth suppression in oxygen-rich metal oxide nanoribbons. Science Advances, 2021, 7, eabh2012.	10.3	12
24	Synergistic Integration of Chemoâ€Resistive and SERS Sensing for Labelâ€Free Multiplex Gas Detection (Adv. Mater. 44/2021). Advanced Materials, 2021, 33, 2170350.	21.0	1
25	Current-induced manipulation of exchange bias in IrMn/NiFe bilayer structures. Nature Communications, 2021, 12, 6420.	12.8	24
26	Polarized ultraviolet emitters with Al wire-grid polarizers fabricated by solvent-assisted nanotransfer process. Nanotechnology, 2020, 31, 045304.	2.6	3
27	Cascade surface modification of colloidal quantum dot inks enables efficient bulk homojunction photovoltaics. Nature Communications, 2020, 11, 103.	12.8	181
28	Cascade domino lithography for extreme photon squeezing. Materials Today, 2020, 39, 89-97.	14.2	29
29	Template Dissolution Interfacial Patterning of Single Colloids for Nanoelectrochemistry and Nanosensing. ACS Nano, 2020, 14, 17693-17703.	14.6	25
30	Metallic Woodpile Nanostructures for Femtomolar Sensing of Alzheimer's Neurofilament Lights. ACS Nano, 2020, 14, 10376-10384.	14.6	10
31	Thermally assisted nanotransfer printing with sub–20-nm resolution and 8-inch wafer scalability. Science Advances, 2020, 6, eabb6462.	10.3	35
32	Simulation and Fabrication of Nanoscale Spirals Based on Dual-Scale Self-Assemblies. ACS Applied Materials & Interfaces, 2020, 12, 46678-46685.	8.0	7
33	Highly Efficient Deep Blue Cdâ€Free Quantum Dot Lightâ€Emitting Diodes by a pâ€Type Doped Emissive Layer. Small, 2020, 16, e2002109.	10.0	24
34	Enhanced flux of chemically induced hot electrons on a Pt nanowire/Si nanodiode during decomposition of hydrogen peroxide. Nanoscale Advances, 2020, 2, 4410-4416.	4.6	6
35	Desolvationâ€Triggered Versatile Transferâ€Printing of Pure BN Films with Thermal–Optical Dual Functionality. Advanced Materials, 2020, 32, 2002099.	21.0	5
36	Engineering Nanoscale Interfaces of Metal/Oxide Nanowires to Control Catalytic Activity. ACS Nano, 2020, 14, 8335-8342.	14.6	22

Yeon Sik Jung

#	Article	IF	CITATIONS
37	Thermodynamic-driven polychromatic quantum dot patterning for light-emitting diodes beyond eye-limiting resolution. Nature Communications, 2020, 11, 3040.	12.8	53
38	Selective, Quantitative, and Multiplexed Surfaceâ€Enhanced Raman Spectroscopy Using Aptamerâ€Functionalized Monolithic Plasmonic Nanogrids Derived from Crossâ€Point Nanoâ€Welding. Advanced Functional Materials, 2020, 30, 2000612.	14.9	25
39	Carboxylic Acid-Functionalized, Graphitic Layer-Coated Three-Dimensional SERS Substrate for Label-Free Analysis of Alzheimer's Disease Biomarkers. Nano Letters, 2020, 20, 2576-2584.	9.1	64
40	Fabrication and Applications of 3D Nanoarchitectures for Advanced Electrocatalysts and Sensors. Advanced Materials, 2020, 32, e1907500.	21.0	17
41	Highly efficient oxygen evolution reaction via facile bubble transport realized by three-dimensionally stack-printed catalysts. Nature Communications, 2020, 11, 4921.	12.8	93
42	Surface wrinkle formation by liquid crystalline polymers for significant light extraction enhancement on quantum dot light-emitting diodes. Optics Express, 2020, 28, 26519.	3.4	7
43	Scalable Nanofabrication of Plasmonic Nanostructures for Trace-Amount Molecular Sensing Based on Surface-Enhanced Raman Spectroscopy (SERS). , 2020, , 71-92.		0
44	Individual Confinement of Block Copolymer Microdomains in Nanoscale Crossbar Templates. Advanced Functional Materials, 2019, 29, 1805795.	14.9	12
45	Regioregularity controlled phase behavior for Poly(3-hexylthiophene): A combined study of simple coarse-grained simulation and experiment. Polymer, 2019, 178, 121569.	3.8	1
46	Ultrasensitive MoS2 photodetector by serial nano-bridge multi-heterojunction. Nature Communications, 2019, 10, 4701.	12.8	66
47	Suppressing Interfacial Dipoles to Minimize Openâ€Circuit Voltage Loss in Quantum Dot Photovoltaics. Advanced Energy Materials, 2019, 9, 1901938.	19.5	14
48	Universal Synthesis of Porous Inorganic Nanosheets via Graphene-Cellulose Templating Route. ACS Applied Materials & Interfaces, 2019, 11, 34100-34108.	8.0	13
49	Order-of-Magnitude, Broadband-Enhanced Light Emission from Quantum Dots Assembled in Multiscale Phase-Separated Block Copolymers. Nano Letters, 2019, 19, 6827-6838.	9.1	21
50	Natural-Wood-Derived Lignosulfonate Ionomer as Multifunctional Binder for High-Performance Lithium–Sulfur Battery. ACS Sustainable Chemistry and Engineering, 2019, 7, 17580-17586.	6.7	43
51	Tuning Soluteâ€Redistribution Dynamics for Scalable Fabrication of Colloidal Quantumâ€Dot Optoelectronics. Advanced Materials, 2019, 31, e1805886.	21.0	28
52	Titanium(III) Sulfide Nanoparticles Coated with Multicomponent Oxide (Ti–S–O) as a Conductive Polysulfide Scavenger for Lithium–Sulfur Batteries. Electronic Materials Letters, 2019, 15, 613-622.	2.2	4
53	Siloxane-Encapsulated Upconversion Nanoparticle Hybrid Composite with Highly Stable Photoluminescence against Heat and Moisture. ACS Applied Materials & Interfaces, 2019, 11, 15952-15959.	8.0	13
54	Versatile, transferrable 3-dimensionally nanofabricated Au catalysts with high-index crystal planes for highly efficient and robust electrochemical CO ₂ reduction. Journal of Materials Chemistry A, 2019, 7, 6045-6052.	10.3	28

#	Article	IF	CITATIONS
55	Nanopatterned High-Frequency Supporting Structures Stably Eliminate Substrate Effects Imposed on Two-Dimensional Semiconductors. Nano Letters, 2018, 18, 2893-2902.	9.1	3
56	Photoâ€Reconfigurable Azopolymer Etch Mask: Photofluidizationâ€Driven Reconfiguration and Edge Rectangularization. Small, 2018, 14, e1703250.	10.0	10
57	Palladiumâ€Đecorated Silicon Nanomesh Fabricated by Nanosphere Lithography for High Performance, Room Temperature Hydrogen Sensing. Small, 2018, 14, 1703691.	10.0	52
58	Synthesis of colloidal VO2 nanoparticles for thermochromic applications. Solar Energy Materials and Solar Cells, 2018, 176, 266-272.	6.2	28
59	Transferrable Plasmonic Au Thin Film Containing Sub-20 nm Nanohole Array Constructed via High-Resolution Polymer Self-Assembly and Nanotransfer Printing. ACS Applied Materials & Interfaces, 2018, 10, 2216-2223.	8.0	22
60	Extremely Small Pyrrhotite Fe ₇ S ₈ Nanocrystals with Simultaneous Carbonâ€Encapsulation for Highâ€Performance Na–Ion Batteries. Small, 2018, 14, 1702816.	10.0	62
61	Thermodynamic and Kinetic Tuning of Block Copolymer Based on Random Copolymerization for Highâ€Quality Subâ€6 nm Pattern Formation. Advanced Functional Materials, 2018, 28, 1800765.	14.9	23
62	Spontaneous Registration of Sub-10 nm Features Based on Subzero Celsius Spin-Casting of Self-Assembling Building Blocks Directed by Chemically Encoded Surfaces. ACS Nano, 2018, 12, 8224-8233.	14.6	6
63	Engraving High-Density Nanogaps in Gold Thin Films via Sequential Anodization and Reduction for Surface-Enhanced Raman Spectroscopy Applications. Chemistry of Materials, 2018, 30, 6183-6191.	6.7	12
64	Plasmonâ€Enhanced Photodetection in Ferromagnet/Nonmagnet Spin Thermoelectric Structures. Advanced Functional Materials, 2018, 28, 1802936.	14.9	7
65	Molecular structure engineering of dielectric fluorinated polymers for enhanced performances of triboelectric nanogenerators. Nano Energy, 2018, 53, 37-45.	16.0	47
66	Direct Fabrication of Micro/Nano-Patterned Surfaces by Vertical-Directional Photofluidization of Azobenzene Materials. ACS Nano, 2017, 11, 1320-1327.	14.6	55
67	Area-Selective Lift-Off Mechanism Based on Dual-Triggered Interfacial Adhesion Switching: Highly Facile Fabrication of Flexible Nanomesh Electrode. ACS Nano, 2017, 11, 3506-3516.	14.6	33
68	Effective Suppression of Polysulfide Dissolution by Uniformly Transfer-Printed Conducting Polymer on Sulfur Cathode for Li-S Batteries. Journal of the Electrochemical Society, 2017, 164, A6417-A6421.	2.9	26
69	Regioregularity-Driven Morphological Transition of Poly(3-hexylthiophene)-Based Block Copolymers. Macromolecules, 2017, 50, 1902-1908.	4.8	34
70	Glyoxalated polyacrylamide as a covalently attachable and rapidly cross-linkable binder for Si electrode in lithium ion batteries. Electronic Materials Letters, 2017, 13, 136-141.	2.2	10
71	Interfacial Energy-Controlled Top Coats for Gyroid/Cylinder Phase Transitions of Polystyrene- <i>block</i> -polydimethylsiloxane Block Copolymer Thin Films. ACS Applied Materials & Interfaces, 2017, 9, 17427-17434.	8.0	14
72	Atomic Layer Etching Mechanism of MoS ₂ for Nanodevices. ACS Applied Materials & Interfaces, 2017, 9, 11967-11976.	8.0	81

Yeon Sik Jung

#	Article	IF	CITATIONS
73	Interfacial band-edge engineered TiO2 protection layer on Cu2O photocathodes for efficient water reduction reaction. Electronic Materials Letters, 2017, 13, 57-65.	2.2	33
74	Synthesis of poly(styrene- <i>b</i> -4-(<i>tert</i> -butyldimethylsiloxy)styrene) block copolymers and characterization of their self-assembled patterns. Molecular Systems Design and Engineering, 2017, 2, 589-596.	3.4	6
75	Long-Term Stable 2H-MoS ₂ Dispersion: Critical Role of Solvent for Simultaneous Phase Restoration and Surface Functionalization of Liquid-Exfoliated MoS ₂ . ACS Omega, 2017, 2, 4678-4687.	3.5	55
76	Flexible and Robust Superomniphobic Surfaces Created by Localized Photofluidization of Azopolymer Pillars. ACS Nano, 2017, 11, 7821-7828.	14.6	115
77	Nanotransplantation Printing of Crystallographic-Orientation-Controlled Single-Crystalline Nanowire Arrays on Diverse Surfaces. ACS Nano, 2017, 11, 11642-11652.	14.6	16
78	Highly Asymmetric n ⁺ –p Heterojunction Quantumâ€Dot Solar Cells with Significantly Improved Chargeâ€Collection Efficiencies. Advanced Materials, 2016, 28, 1780-1787.	21.0	29
79	Surfaceâ€Shielding Nanostructures Derived from Selfâ€Assembled Block Copolymers Enable Reliable Plasma Doping for Few‣ayer Transition Metal Dichalcogenides. Advanced Functional Materials, 2016, 26, 5631-5640.	14.9	19
80	Reliable Memristive Switching Memory Devices Enabled by Densely Packed Silver Nanocone Arrays as Electric-Field Concentrators. ACS Nano, 2016, 10, 9478-9488.	14.6	90
81	3D Crossâ€Point Plasmonic Nanoarchitectures Containing Dense and Regular Hot Spots for Surfaceâ€Enhanced Raman Spectroscopy Analysis. Advanced Materials, 2016, 28, 8695-8704.	21.0	178
82	Fabrication of 50 nm scale Pt nanostructures by block copolymer (BCP) and its characteristics of surface-enhanced Raman scattering (SERS). RSC Advances, 2016, 6, 70756-70762.	3.6	11
83	Block Copolymer with an Extremely High Block-to-Block Interaction for a Significant Reduction of Line-Edge Fluctuations in Self-Assembled Patterns. Chemistry of Materials, 2016, 28, 5680-5688.	6.7	32
84	In Situ Nanolithography with Subâ€10 nm Resolution Realized by Thermally Assisted Spin asting of a Selfâ€Assembling Polymer. Advanced Materials, 2015, 27, 4814-4822.	21.0	20
85	Eliminating the Tradeâ€Off between the Throughput and Pattern Quality of Subâ€15 nm Directed Selfâ€Assembly via Warm Solvent Annealing. Advanced Functional Materials, 2015, 25, 306-315.	14.9	49
86	Sequentially Self-Assembled Rings-in-Mesh Nanoplasmonic Arrays for Surface-Enhanced Raman Spectroscopy. Chemistry of Materials, 2015, 27, 5007-5013.	6.7	28
87	Self-Extinguishing Lithium Ion Batteries Based on Internally Embedded Fire-Extinguishing Microcapsules with Temperature-Responsiveness. Nano Letters, 2015, 15, 5059-5067.	9.1	101
88	Hierarchically Self-Assembled Block Copolymer Blends for Templating Hollow Phase-Change Nanostructures with an Extremely Low Switching Current. Chemistry of Materials, 2015, 27, 2673-2677.	6.7	11
89	Flexible One Diode-One Phase Change Memory Array Enabled by Block Copolymer Self-Assembly. ACS Nano, 2015, 9, 4120-4128.	14.6	74
90	Enhancing the Directed Self-assembly Kinetics of Block Copolymers Using Binary Solvent Mixtures. ACS Applied Materials & Interfaces, 2015, 7, 25843-25850.	8.0	18

#	Article	IF	CITATIONS
91	Controlled Doping of Vacancy-Containing Few-Layer MoS ₂ <i>via</i> Highly Stable Thiol-Based Molecular Chemisorption. ACS Nano, 2015, 9, 12115-12123.	14.6	320
92	Single Nanoparticle Localization in the Perforated Lamellar Phase of Self-Assembled Block Copolymer Driven by Entropy Minimization. Macromolecules, 2015, 48, 7938-7944.	4.8	11
93	Soft Patchy Particles of Block Copolymers from Interface-Engineered Emulsions. ACS Nano, 2015, 9, 11333-11341.	14.6	91
94	Longâ€Range Ordered Selfâ€Assembly of Novel Acrylamideâ€Based Diblock Copolymers for Nanolithography and Metallic Nanostructure Fabrication. Advanced Materials, 2014, 26, 2894-2900.	21.0	10
95	Topographically-Designed Triboelectric Nanogenerator via Block Copolymer Self-Assembly. Nano Letters, 2014, 14, 7031-7038.	9.1	310
96	High-resolution nanotransfer printing applicable to diverse surfaces via interface-targeted adhesion switching. Nature Communications, 2014, 5, 5387.	12.8	178
97	Tailoring of the PbS/metal interface in colloidal quantum dot solar cells for improvements of performance and air stability. Energy and Environmental Science, 2014, 7, 3052.	30.8	55
98	Reliable Control of Filament Formation in Resistive Memories by Self-Assembled Nanoinsulators Derived from a Block Copolymer. ACS Nano, 2014, 8, 9492-9502.	14.6	93
99	Deep-Nanoscale Pattern Engineering by Immersion-Induced Self-Assembly. ACS Nano, 2014, 8, 10009-10018.	14.6	46
100	Threeâ€Dimensional Nanofabrication by Block Copolymer Selfâ€Assembly. Advanced Materials, 2014, 26, 4386-4396.	21.0	155
101	Extremely High Yield Conversion from Lowâ€Cost Sand to Highâ€Capacity Si Electrodes for Liâ€lon Batteries. Advanced Energy Materials, 2014, 4, 1400622.	19.5	75
102	Proximity Injection of Plasticizing Molecules to Self-Assembling Polymers for Large-Area, Ultrafast Nanopatterning in the Sub-10-nm Regime. ACS Nano, 2013, 7, 6747-6757.	14.6	70
103	Host-Guest Self-assembly in Block Copolymer Blends. Scientific Reports, 2013, 3, 3190.	3.3	34
104	Porous silicon nanowires for lithium rechargeable batteries. Nanotechnology, 2013, 24, 424008.	2.6	38
105	Ultraâ€High Optical Transparency of Robust, Gradedâ€Index, and Antiâ€Fogging Silica Coating Derived from Siâ€Containing Block Copolymers. Advanced Optical Materials, 2013, 1, 428-433.	7.3	29
106	Localized surface plasmon-enhanced nanosensor platform using dual-responsive polymer nanocomposites. Nanoscale, 2013, 5, 7403.	5.6	16
107	Self-Assembled Incorporation of Modulated Block Copolymer Nanostructures in Phase-Change Memory for Switching Power Reduction. ACS Nano, 2013, 7, 2651-2658.	14.6	74
108	Li ₃ V ₂ (PO ₄) ₃ /Conducting Polymer as a High Power 4 Vâ€Class Lithium Battery Electrode. Advanced Energy Materials, 2013, 3, 1004-1007.	19.5	75

#	Article	IF	CITATIONS
109	Current density enhancement nano-contact phase-change memory for low writing current. Applied Physics Letters, 2013, 103, .	3.3	8
110	Low Power Phase Change Memory via Block Copolymer Self-assembly Technology. Materials Research Society Symposia Proceedings, 2013, 1556, 1.	0.1	0
111	Uniform Graphene Quantum Dots Patterned from Self-Assembled Silica Nanodots. Nano Letters, 2012, 12, 6078-6083.	9.1	186
112	Self-Assembly-Induced Formation of High-Density Silicon Oxide Memristor Nanostructures on Graphene and Metal Electrodes. Nano Letters, 2012, 12, 1235-1240.	9.1	89
113	Layer-structured phase-segregation of red-emitting quantum dots from green-emitting small molecule-embedded polymer film. Macromolecular Research, 2012, 20, 1121-1123.	2.4	0
114	Tailored Li4Ti5O12 nanofibers with outstanding kinetics for lithium rechargeable batteries. Nanoscale, 2012, 4, 6870.	5.6	74
115	Lithiumâ€lon Batteries: A Stretchable Polymer–Carbon Nanotube Composite Electrode for Flexible Lithiumâ€lon Batteries: Porosity Engineering by Controlled Phase Separation (Adv. Energy Mater. 8/2012). Advanced Energy Materials, 2012, 2, 914-914.	19.5	1
116	Directed Selfâ€Assembly with Subâ€100 Degrees Celsius Processing Temperature, Subâ€10 Nanometer Resolution, and Subâ€1 Minute Assembly Time. Small, 2012, 8, 3762-3768.	10.0	81
117	Nanotransfer Printing with subâ€10 nm Resolution Realized using Directed Selfâ€Assembly. Advanced Materials, 2012, 24, 3526-3531.	21.0	91
118	Scalable Fabrication of Silicon Nanotubes and their Application to Energy Storage. Advanced Materials, 2012, 24, 5452-5456.	21.0	338
119	A Stretchable Polymer–Carbon Nanotube Composite Electrode for Flexible Lithiumâ€ion Batteries: Porosity Engineering by Controlled Phase Separation. Advanced Energy Materials, 2012, 2, 976-982.	19.5	141
120	Highly Tunable Self-Assembled Nanostructures from a Poly(2-vinylpyridine- <i>b</i> -dimethylsiloxane) Block Copolymer. Nano Letters, 2011, 11, 4095-4101.	9.1	202
121	Complex self-assembled patterns using sparse commensurate templates with locally varying motifs. Nature Nanotechnology, 2010, 5, 256-260.	31.5	245
122	A Path to Ultranarrow Patterns Using Self-Assembled Lithography. Nano Letters, 2010, 10, 1000-1005.	9.1	229
123	Nanoimprint-Induced Molecular Stacking and Pattern Stabilization in a Solution-Processed Subphthalocyanine Film. ACS Nano, 2010, 4, 2627-2634.	14.6	14
124	Enhancing the Potential of Block Copolymer Lithography with Polymer Self-Consistent Field Theory Simulations. Macromolecules, 2010, 43, 8290-8295.	4.8	38
125	Formation of Bandgap and Subbands in Graphene Nanomeshes with Sub-10 nm Ribbon Width Fabricated via Nanoimprint Lithography. Nano Letters, 2010, 10, 2454-2460.	9.1	302
126	Fabrication of Diverse Metallic Nanowire Arrays Based on Block Copolymer Self-Assembly. Nano Letters, 2010, 10, 3722-3726.	9.1	102

#	Article	IF	CITATIONS
127	Solventâ€Vaporâ€Induced Tunability of Selfâ€Assembled Block Copolymer Patterns. Advanced Materials, 2009, 21, 2540-2545.	21.0	238
128	Negative thermal quenching in undoped ZnO and Ga-doped ZnO film grown on c-Al2O3 (0001) by plasma-assisted molecular beam epitaxy. Journal of Electroceramics, 2009, 23, 331-334.	2.0	4
129	Cobalt Nanoparticle Arrays made by Templated Solid‧tate Dewetting. Small, 2009, 5, 860-865.	10.0	98
130	Wellâ€Ordered Thinâ€Film Nanopore Arrays Formed Using a Blockâ€Copolymer Template. Small, 2009, 5, 1654-1659.	10.0	75
131	Nanofabricated Concentric Ring Structures by Templated Self-Assembly of a Diblock Copolymer. Nano Letters, 2008, 8, 2975-2981.	9.1	117
132	Nanowire Conductive Polymer Gas Sensor Patterned Using Self-Assembled Block Copolymer Lithography. Nano Letters, 2008, 8, 3776-3780.	9.1	197
133	Graphoepitaxy of Self-Assembled Block Copolymers on Two-Dimensional Periodic Patterned Templates. Science, 2008, 321, 939-943.	12.6	760
134	Controlling the Morphology of Side Chain Liquid Crystalline Block Copolymer Thin Films through Variations in Liquid Crystalline Content. Nano Letters, 2008, 8, 3434-3440.	9.1	46
135	Si-containing block copolymers for self-assembled nanolithography. Journal of Vacuum Science & Technology B, 2008, 26, 2489-2494.	1.3	82
136	Photoluminescence of Ga-doped ZnO film grown on c-Al2O3 (0001) by plasma-assisted molecular beam epitaxy. Journal of Applied Physics, 2007, 102, .	2.5	40
137	Orientation-Controlled Self-Assembled Nanolithography Using a Polystyreneâ^'Polydimethylsiloxane Block Copolymer. Nano Letters, 2007, 7, 2046-2050.	9.1	424
138	Chemical reaction of sputtered Cu film with PI modified by low energy reactive atomic beam. Applied Surface Science, 2006, 252, 5877-5891.	6.1	107
139	Dependences of the surface and the optical properties on the O2/O2+Ar flow-rate ratios for ZnO thin films grown on ZnO buffer layers. Applied Surface Science, 2006, 252, 8121-8125.	6.1	4
140	Electron transport in high quality undoped ZnO film grown by plasma-assisted molecular beam epitaxy. Solid State Communications, 2006, 137, 474-477.	1.9	16
141	Enhancement of the surface and structural properties of ZnO epitaxial films grown on Al2O3 substrates utilizing annealed ZnO buffer layers. Journal of Electroceramics, 2006, 17, 283-285.	2.0	2
142	Luminescence of bound excitons in epitaxial ZnO thin films grown by plasma-assisted molecular beam epitaxy. Journal of Applied Physics, 2006, 99, 013502.	2.5	40
143	Ferromagnetism in 200-MeV Ag+15-ion-irradiated Co-implanted ZnO thin films. Applied Physics Letters, 2006, 88, 142502.	3.3	47
144	A stationary plasma thruster for modification of polymer and ceramic surfaces. Nuclear Instruments & Methods in Physics Research B, 2005, 239, 440-450.	1.4	11

#	Article	IF	CITATIONS
145	Two-dimensional growth of ZnO epitaxial films on c-Al2O3 (0001) substrates with optimized growth temperature and low-temperature buffer layer by plasma-assisted molecular beam epitaxy. Journal of Crystal Growth, 2005, 274, 418-424.	1.5	35
146	Growth and properties of ZnO nanoblade and nanoflower prepared by ultrasonic pyrolysis. Journal of Applied Physics, 2005, 97, 044305.	2.5	67
147	A spectroscopic ellipsometry study on the variation of the optical constants of tin-doped indium oxide thin films during crystallization. Solid State Communications, 2004, 129, 491-495.	1.9	30
148	Influence of dc magnetron sputtering parameters on surface morphology of indium tin oxide thin films. Applied Surface Science, 2004, 221, 136-142.	6.1	91
149	Study on texture evolution and properties of silver thin films prepared by sputtering deposition. Applied Surface Science, 2004, 221, 281-287.	6.1	60
150	Spectroscopic ellipsometry studies on the optical constants of indium tin oxide films deposited under various sputtering conditions. Thin Solid Films, 2004, 467, 36-42.	1.8	90
151	The effect of ZnO homo-buffer layer on ZnO thin films grown on c-Al2O3(0001) by plasma assisted molecular beam epitaxy. Journal of Crystal Growth, 2004, 267, 85-91.	1.5	22
152	Development of indium tin oxide film texture during DC magnetron sputtering deposition. Journal of Crystal Growth, 2003, 259, 343-351.	1.5	77
153	Influence of DC magnetron sputtering parameters on the properties of amorphous indium zinc oxide thin film. Thin Solid Films, 2003, 445, 63-71.	1.8	202
154	Effects of thermal treatment on the electrical and optical properties of silver-based indium tin oxide structures. Thin Solid Films, 2003, 440, 278-284.	1.8	97
155	Surface structure and field emission property of carbon nanotubes grown by radio-frequency plasma-enhanced chemical vapor deposition. Applied Surface Science, 2002, 193, 129-137,	6.1	30